Supplemental Table of Contents

Supplemental Table 1. Primer sequences. Shown are sequences of primer sets used for the expression analysis of the indicated genes by RT-PCR.

Gene	**Forward Primer** **Reverse Primer**
Kim1 (mouse)	5′-AAACCAGAGATTCCCACACG-3′ 5′-GTCGTGGGTCTTCCTGTAGC-3′
Loxl2 (mouse)	5′-GATCTTCAGCCCCGATGGA-3′ 5′-CAAGGGTTGCTCTGGCTTGT-3′
Tgfβ1 (mouse)	5′-TGGCGAGCCTTAGTTTGGA-3′ 5′-TCGACATGGAGCTGGTGAAA-3′
Acta2 (mouse)	5′-CCTGACGCTGAAGTATCCGATAG-3′ 5′-TTTTCCATGTCGTCCCAGTTG-3′
Pgk1 (mouse)	5′-CAAACAACCAAAGGATCAAGG-3′ 5′-CCCAAGATAGCCAGGAAGG-3′
Pdk1 (mouse)	5′-GTTAGGGATAGGGTTGGAGATCTTT-3′ 5′-TCACAGGATGGTTGGTTCTTTCT-3′
Ldha (mouse)	5´-CGTCTCCCTGAAGTCTCTTAACC-3´ 5´-CCCACACCATCTCAACACC-3´
Kdr (mouse)	5´-ACTGCAGTGATTGCCATGTTCT-3´ 5´-TCATTGGCCCGCTTAACG-3´
Emcn (mouse)	5´-TGCAACCACTCCATCAACCA-3´ 5´-CGCGATAACCACAGGCAAA-3´
Vcam1 (mouse)	5´-TAGAGTGCAAGGAGTTCGGG-3´ 5´-CCGGCATATACGAGTGTGAA-3´
Icam1 (mouse)	5´-TGGATACCTGAGCATCACCA-3´ 5´-CTGCTACCTGCACTTTGCC-3´
Cxcl1 (mouse)	5´-GCAGACCATGGCTGGGATT-3′ 5´-CCTGAGGGCAACACCTTCAA-3′

Cxcl2 (mouse)	5´-GCGCCCAGACAGAAGTCATAG-3′ 5´-AGGGTCAAGGCAAACTTTTTGA-3′
Tnfa (mouse)	5´-GCTGAGCTCAAACCCTGGTA-3′ 5´-CGGACTCCGCAAAGTCTAAG-3′
VCAM1 (human)	5´-GCTTCAGGAGCTGAATACCC-3′ 5´-AAGGATCACGACCATCTTCC-3′
IRF-1 (human)	5´-TTTCGCTGTGCCATGAACTC-3′ 5´-TGTTCCTGCTCTGGTCTTTCAC-3′

Supplemental Figure 1. **Validation of *Cdh5-Cre* driven recombination of the *Phd2* flox allele in the kidney**. Recombination analysis of *Phd2* flox allele in genomic DNA isolated from kidneys of *EC-Phd2* mice or their *Cre*- littermate controls. Primers used, amplify the conditional (2-lox) and the recombined (1-lox) allele.

Supplemental Figure 2. Endothelial *Phd2* ablation does not alter serum BUN levels 1 day following bilateral IRI. Shown are serum BUN levels in *EC-Phd2* mice or their *Cre*- littermate controls at day 1 after bilateral IRI (n=16-17; P>0.5, 2-tailed Student's t-test). ns, not statistically significant

Supplemental Figure 3. Endothelial *Phd2* deletion does not alter post-ischemic kidney stabilization of HIF at day 3 post unilateral renal IRI. **(A)** Shown is immunoblot analysis of HIF-1α and HIF-2α in post-ischemic kidneys from *EC-Phd2* and *Cre*- controls at day 3 post unilateral renal IRI. Ponceau S staining was used to assess for equal protein loading. Nuclear kidney extracts from a mouse treated with an oral PHD inhibitor served as positive control (+Co). Right graphs show densitometric analyses of HIF-1α and HIF-2α normalized to Ponceau. **(B)** Representative images of immunofluorescence detection of HIF-1 on kidney cryosections from *EC-Phd2;mT/mG* and *EC;mT/mG* mice at day 3 following unilateral renal artery clamping compared to uninjured kidneys. Shown are merged images of mTomato (red), EGFP (green) and HIF-1 staining (white) with (top 2 rows) or without DAPI (bottom 2 rows). Non-recombined cells express membrane-bound mTomato while recombined cells express membrane-bound EGFP. In the *EC-Phd2;mT/mG* mice, $EGFP^{+ve}$ cells represent *Phd2* deficient ECs whereas in the *EC;mT/mG* controls, $EGFP^{+ve}$ cells correspond to ECs competent for *Phd2*. Insets, top 2 rows: higher magnification views from dashed square marked areas showing ECs without evidence of HIF

staining. Overall, at day 3 post IRI the staining for HIF-1 was rare and there was no difference in endothelial HIF-1 between mutants and controls. Yellow arrows indicate HIF-1 stained nuclei. Scale bars indicate 50 μm.

Supplemental Figure 4. Single cell transcriptomic analysis of *Phds/Egln*s in kidney endothelial cells. The *t*-distributed stochastic neighbor embedding (tSNE) map demonstrates 16 distinct cell types revealed by unsupervised clustering. Right panel shows the magnified endothelial cell cluster, which consisted 2.29% of 43,745 analyzed cells. Bottom panel depicts heatmap showing the expression levels of *Egln1 (Phd2), Egln2 (Phd1)* and *Egln3 (Phd3)* in kidney endothelial cells. The color scheme is based on z-score distribution.

Supplemental Figure 5. Concurrent endothelial *Phd2 and Hif2* deletion does not alter post-ischemic kidney mRNA levels of *Il-1b* and *Il-6* at day 3 post unilateral renal IRI. Shown are mRNA levels of *Il-1b* and *Il-6* in post-ischemic and contralateral kidneys of *EC-Phd2Hif2* mice and their *Cre-* controls at day 3 post unilateral IRI (n=8; P>0.05, 1-way ANOVA with Sidak correction for multiple comparisons).

Supplemental Figure 6. Inducible endothelial specific inactivation of *Phd2* attenuates histological kidney injury at day 3 following renal IRI. (A) Background autofluorescence indicated by the percentage of GFP^{+ve} cells in bone marrow of *Cre-* (*mT/mG*) mice. **(B)** Recombination analysis of *Phd2* flox allele in genomic DNA isolated from kidney, lung, liver and heart following tamoxifen treatment of *iEC-Phd2* and *Cre-* mice. **(C)** Acute injury scores in post-

ischemic kidneys of tamoxifen treated *iEC-Phd2* and *Cre-* mice at day 3 following kidney IRI (n=5-4; P=0.0446, 2-tailed Student's t-test).

Supplemental Figure 7. Endothelial *Phd2* ablation does not influence serum kynurenic acid and α-ketoglutarate levels. Serum kynurenic acid and α-ketoglutarate levels for *EC-Phd2* and *Cre-* mice measured by LC/MS and GC/MS respectively (n=8, P>0.05, 2-tailed Student's t-test).

Supplemental Figure 1

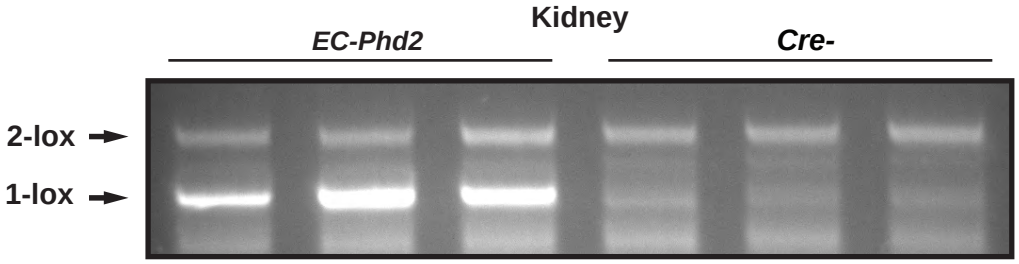

Supplemental Figure 2

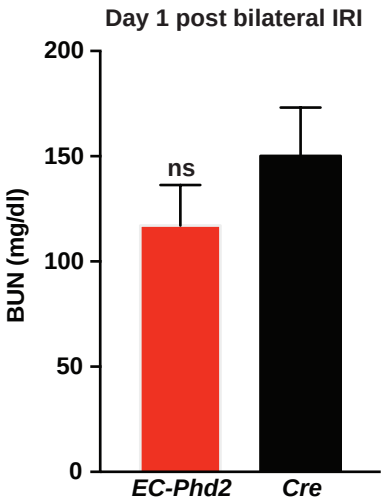

Supplemental Figure 3

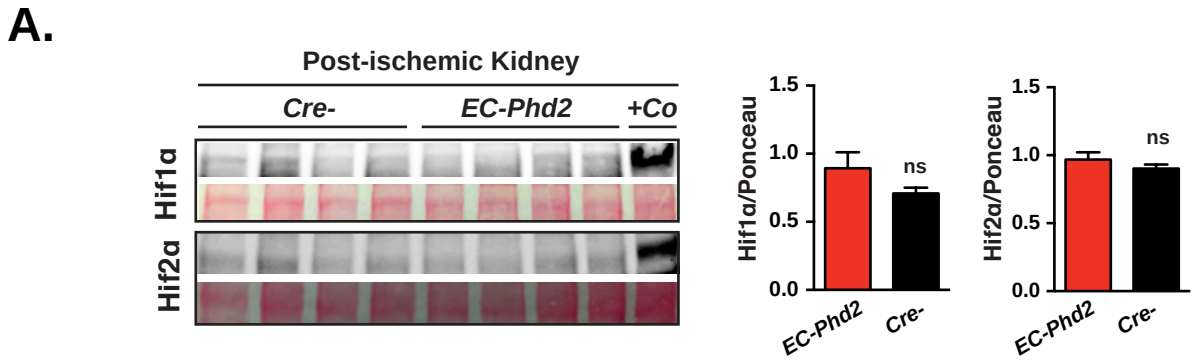

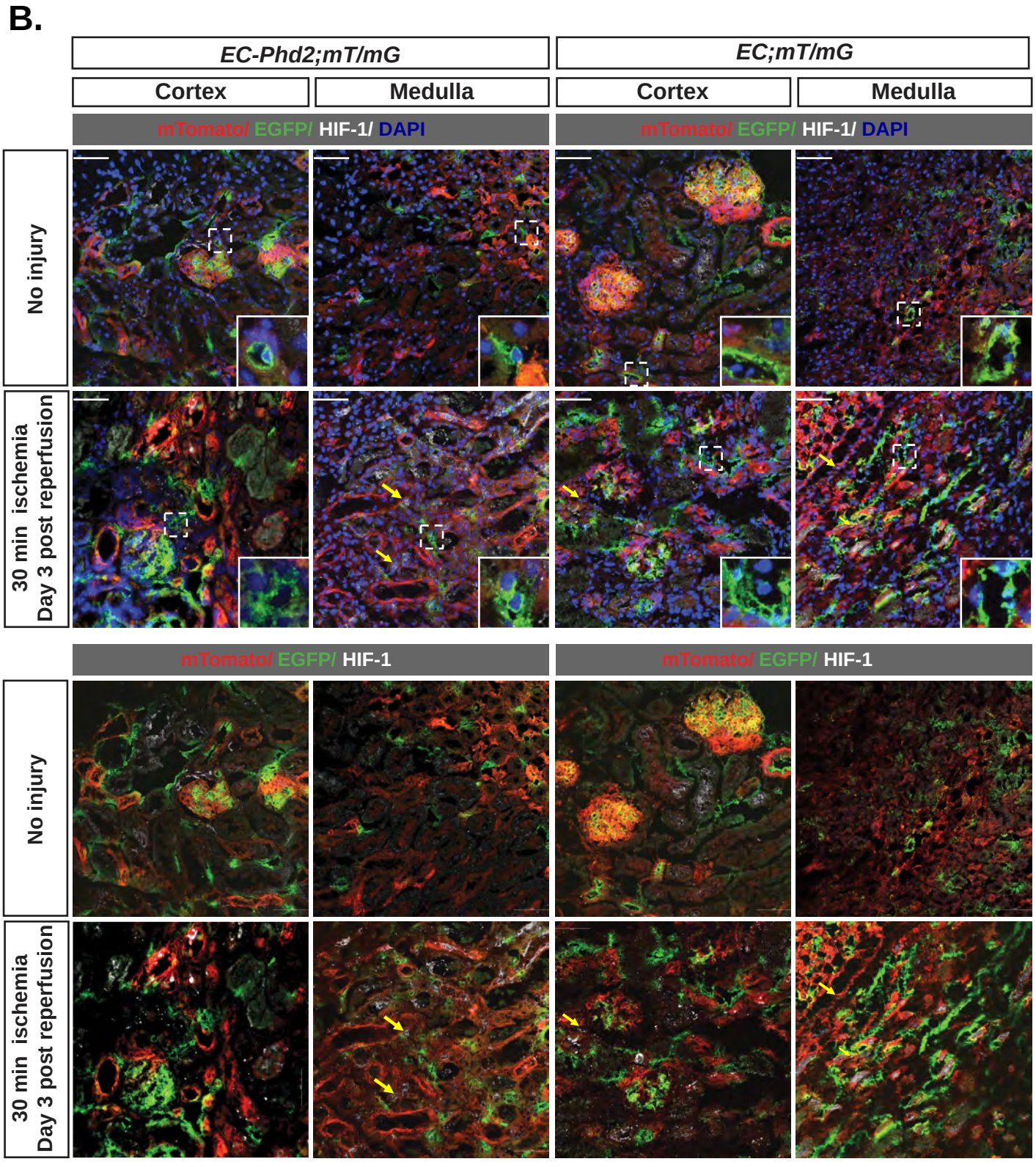

Supplemental Figure 4

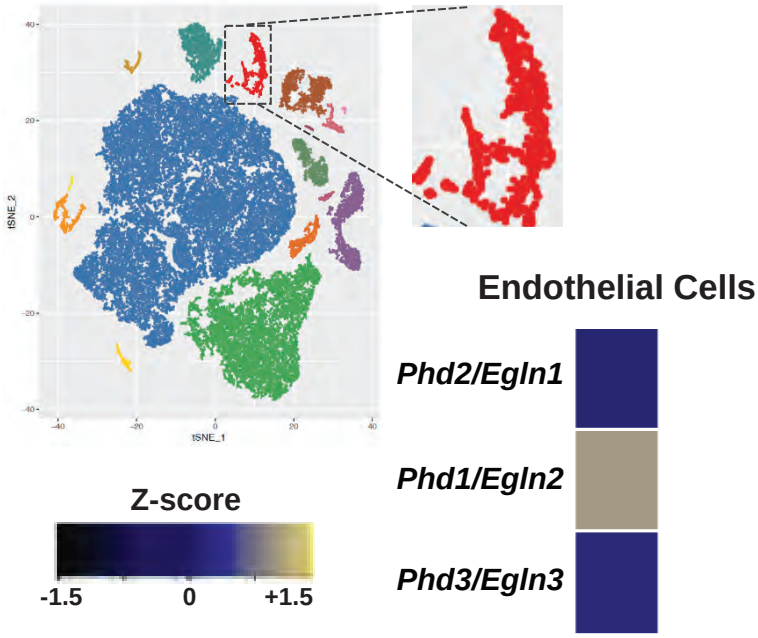

Supplemental Figure 5

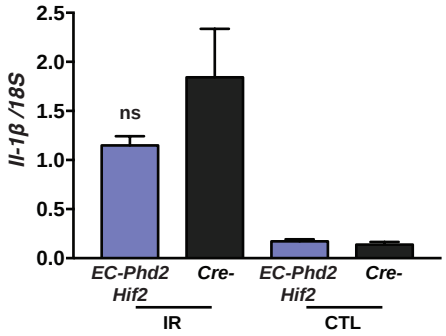

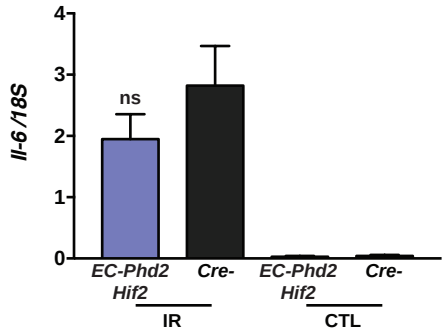

Supplemental Figure 6

A.

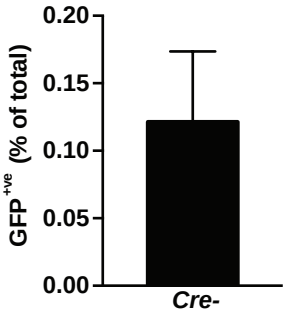

B.

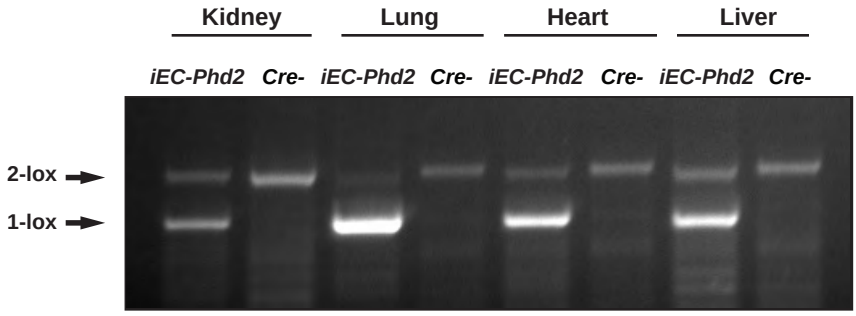

C.

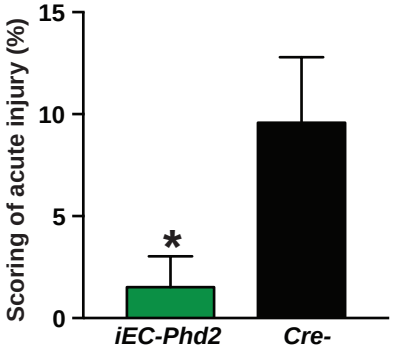

Supplemental Figure 7